machines

MDPI

Article

Design of Dual Winding Flux Modulation Machine for Performance Improvement in Variable Speed Application

Min-Gu Lyeo [1], Kyu-Yun Hwang [2] and Sung-Hyun Lee [3,*]

[1] Control System Research Team, KCNC, Gunpo 15880, Republic of Korea; mglyeo@kcnc.co.kr
[2] School of Electronic Engineering, Kumoh National Institute of Technology, Gumi 39177, Republic of Korea; kyuyun7@kumoh.ac.kr
[3] Intelligent Mechatronics Research Center, Korea Electronics Technology Institute, Bucheon 14502, Republic of Korea
* Correspondence: dltjdgus9417@gmail.com

Abstract: In this paper, a Dual Winding Flux Modulation Machine (DWFMM) is proposed for variable speed application. The DWFMM is configured by adding windings to the Single Winding Flux Modulation Machine (SWFMM), consisting of a master winding that drives the motor and a slave winding that enables pole changing and performance enhancement. Through pole changing, the DWFMM can operate as two different machines: a Vernier Machine (VM) for varying speeds and torque operations and a Permanent Magnet Synchronous Machine (PMSM). In the VM mode, flux enhancement is applied to improve torque, and in the PMSM mode, Flux Weakening is applied to increase speed. The characteristics of the two different operating modes were analyzed using the Finite Element Method (FEM) to validate the machine's performance. Finally, the DWFMM and SWFMM were designed and compared as variable speed application machines to confirm their suitability and superiority.

Keywords: dual winding machine; flux modulation; permanent magnet synchronous motor; pole changing; Vernier Machine

Citation: Lyeo, M.-G.; Hwang, K.-Y.; Lee, S.-H. Design of Dual Winding Flux Modulation Machine for Performance Improvement in Variable Speed Application. *Machines* **2024**, *12*, 535. https://doi.org/10.3390/machines12080535

Academic Editor: Hongrui Cao

Received: 29 June 2024
Revised: 29 July 2024
Accepted: 3 August 2024
Published: 6 August 2024

1. Introduction

Washing machines perform two operations: the washing operation and the dehydration operation. The washing operation is performed at low speeds with high torque, while the dehydration operation is performed at high speeds with low torque. Permanent Magnet Synchronous Machines (PMSM) have a high efficiency at high speeds but low efficiency at low speeds, making them suitable for dehydration operations [1–3]. On the other hand, Vernier Machines (VM) have a high efficiency at low speeds but a low efficiency at high speeds, making them suitable for washing operations. In particular, VMs have what is called a magnetic gearing effect, which provides high torque density and high efficiency at low speeds [4–7]. Due to these advantages, extensive research has been conducted, and various topologies have been proposed.

A Single Winding Flux Modulation Machine (SWFMM) was introduced for a variable speed range operation [8]. The SWFMM operates in two modes, VM and PMSM, depending on the change in the rotor pole number caused by the magnetization direction of the Low Coercive Force permanent magnets (LCF PM) [9–18]. However, controlling the magnetization direction of only the LCF PM in the SWFMM with continuous Permanent Magnets was somewhat challenging. To improve the controllability of the LCF PM magnetization direction in the SWFMM, a Consequent Pole structure was proposed for the SWFMM [19].

The Consequent Pole structure is applied by replacing one of the two permanent magnets with iron. Therefore, in the SWFMM, half of the LCF PM and half of the High Coercive Force permanent magnets (HCF PM) are replaced with iron [20]. As a result, the gap between the magnets widens, and the total number of magnets decreases, which improves

the controllability of the LCF PM magnetization direction. Additionally, the Consequent Pole structure reduces machine costs while maintaining sufficient torque density [21,22]. However, in the SWFMM with the Consequent Pole structure, the reduction in magnets and the increase in iron result in an increased terminal voltage [23,24]. Consequently, this leads to inverter capacity limitations and high power consumption issues, ultimately causing speed limitations.

In this paper, a Dual Winding Flux Modulation Machine (DWFMM) for a variable speed application machine is proposed and explained in Section 2. The DWFMM enhances flux in the VM mode and weakens flux in the PMSM mode more effectively than the SWFMM by adding windings to the SWFMM. The working principles of flux enhancement in the VM mode and Flux Weakening in the PMSM mode within the DWFMM are detailed in Section 3. Finally, a performance analysis of the DWFMM using the Finite Element Method (FEM) is presented, and the advantages of the DWFMM are validated in comparison with the SWFMM in washing and dehydration operations in Section 4.

2. Machine Topologies

Figure 1 shows the topology of the SWFMM. The SWFMM uses two types of permanent magnets: HCF PM and LCF PM. Additionally, a Consequent Pole structure is applied, replacing half of the HCF PM and LCF PM with iron. As a result, the gap between the two magnets widens, forming a closed circuit for the LCF PM, which renders magnetization control easier. However, as the amount of magnets decreases, the magnetomotive force (MMF) of the air gap also reduces by half. On the other hand, due to the Consequent Pole structure, the permeance and modulated waves of the machine increase, resulting in an air gap flux density similar to that before applying the Consequent Pole structure. Additionally, the reluctance torque increases due to the salient pole-type rotor structure. Consequently, the torque characteristics relative to the cost improve, and the controllability of the pole changing becomes easier.

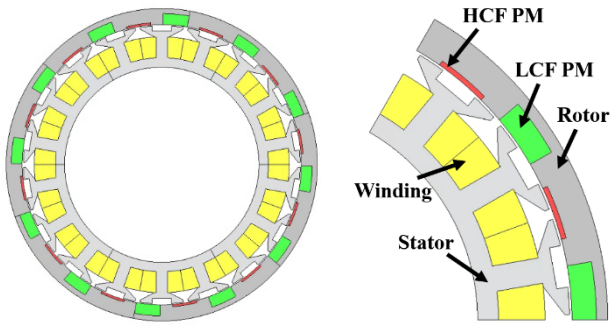

Figure 1. Topology of SWFMM: (**a**) cross-sectional view; (**b**) topology.

However, of the two operating modes of the SWFMM, the terminal voltage increased during the high-speed PMSM operation. Additionally, while the torque characteristics are excellent relative to the cost, the torque itself decreased. To address these shortcomings, the DWFMM in Figure 2 was proposed. In the DWFMM, windings were added between the modulation poles of the SWFMM, and the windings added between the modulation poles are referred to as the slave windings. In this paper, the power for the two additional operating modes proposed is supplied through the slave windings. The windings in the existing slots are referred to as the master windings [25]. The master windings drive the motor using three phases. The slave windings perform pole changing and variable flux control. The variable flux control of the slave windings allows for additional operation in Flux Enhancing and Flux Weakening. By using the modulation poles, the DWFMM has 36 slots and features 12 pole pairs each of HCF PM and LCF PM, totaling 24 pole pairs. The HCF PM has a high coercive force, so to prevent the unintended demagnetization of the

LCF PM, the size of the LCF PM is kept larger than that of the HCF PM. Additionally, the DWFMM uses concentrated windings, resulting in 12 pole pairs. The detailed parameter values of the two machines are shown in Table 1.

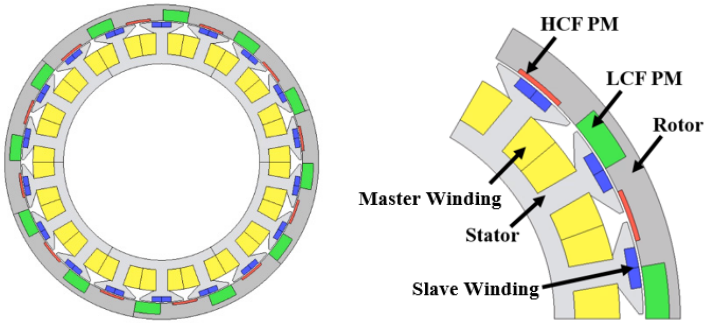

(**a**) (**b**)

Figure 2. Topology of DWFMM: (**a**) cross-sectional view; (**b**) topology.

Table 1. Key parameters.

Parameter Machine Type	Unit	SWFMM VM/PMSM	DWFMM VM/PMSM
Rotor outer diameter	mm	142	142
Air gap length	mm	1	1
Stator outer diameter	mm	125	125
Stator inner diameter	mm	88	88
Stack length	mm	24	24
No. of slot	-	36	36
PM pole pairs	-	24/12	24/12
HCF PM grade	-	NdFeB	NdFeB
LCF PM grade	-	AlNiCo 9	AlNiCo 9

3. Pole Changing

The DWFMM has two operating modes: VM and PMSM. At low speeds, the DWFMM operates as a VM. For the machine to operate as a VM, Equation (1) must be satisfied.

$$Z_r = Z_s - \mathrm{p} \tag{1}$$

where Z_r is the number of rotor pole pairs, Z_s is the number of slots, and p is the number of armature winding pole pairs.

When the DWFMM is operating in VM mode as shown in Figure 3a, the magnetization direction of both the HCF PM and the LCF PM must be the same. Z_r should have 24 pole pairs. Therefore, the operation of the VM satisfies Equation (1) since Z_r, Z_s, and p become 24, 36, and 12, respectively. At high speeds, the proposed DWFMM operates as a PMSM. In order for the proposed DWFMM to operate as a PMSM, Equation (2) must be satisfied.

$$Z_r = \mathrm{p} \tag{2}$$

When operating as a PMSM at high speeds, the magnetizing directions of the HCF PM and LCF PM should be opposite to each other, as illustrated in Figure 3b. Under these conditions, Z_r has 12 pole pairs. Therefore, when operating as a PMSM, Z_r and p both become 12 pole pairs, satisfying Equation (2). In other words, by changing the magnetization direction of the magnets, the number of pole pairs is altered, thereby switching the operation mode from VM to PMSM.

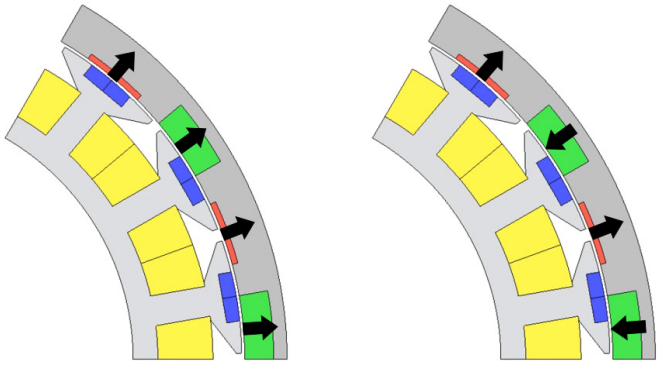

(**a**) (**b**)

Figure 3. Pole changing according to magnetization of PM: (**a**) VM; (**b**) PMSM.

Contrary to constant magnets or HCF PM, LCF PM exhibits a non-linear hysteresis curve, as shown in Figure 4. Initially, the operating point of the LCF PM on the machine is located between points A and B. When the operating point moves below the knee point, irreversible demagnetization occurs, and the flux density of the LCF PM changes along the recoil line curve. The operating point of the LCF PM on the machine is then located between points C and I, resulting in a reduction in the flux density of the LCF PM. However, if a further current in the direction opposite to the magnetization direction, or a negative current, is applied, the operating point can be moved to point D. At that time, the flux density of the LCF PM is zero. If an additional sufficient current is applied in the opposite direction of the initial magnetization of the permanent magnet, the operating point of the LCF PM moves to point F, and the magnetic flux density is between points F and G. This process is called pole changing, and it transitions the machine from the VM operation to the PMSM operation. The method for changing from the PMSM operation to the VM operation is the opposite of the previous method.

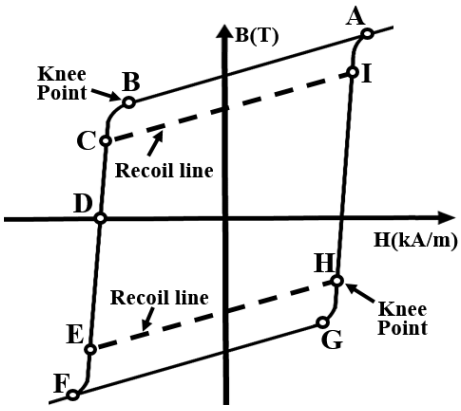

Figure 4. Hysteresis curve of LCF PM.

When the LCF PM is positioned between the slave windings, the pole changing proceeds. At that time, the LCF PM forms a closed circuit. Figure 5 shows that the DWFMM initially operates in the VM mode at a speed of 50 RPM. The slave winding of the DWFMM is supplied with a negative DC of 50 A for pole changing, and the pole-changing current is applied twice. Afterward, the DWFMM transitions from the VM operation to the PMSM operation, as shown in Figure 5, and this can be confirmed through the waveform of the back electromotive force (EMF).

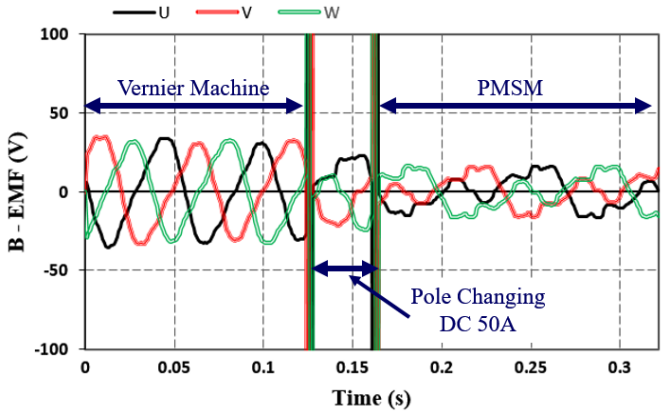

Figure 5. Pole changing of DWFMM for VM to PMSM.

Conversely, Figure 6 shows that the DWFMM changes from the PMSM operation to the VM operation. The slave winding is supplied with twice 50 A DC for pole changing.

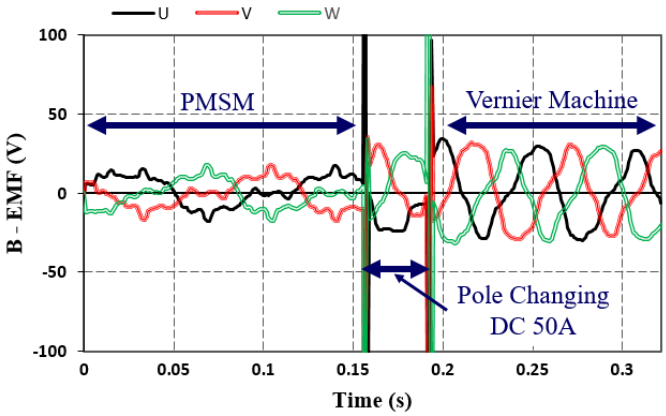

Figure 6. Pole changing of DWFMM for PMSM to VM.

In addition, Figure 7 shows that the magnetization direction of the LCF PM is changed from the VM operation in Figure 7a to the PMSM operation in Figure 7b through pole changing.

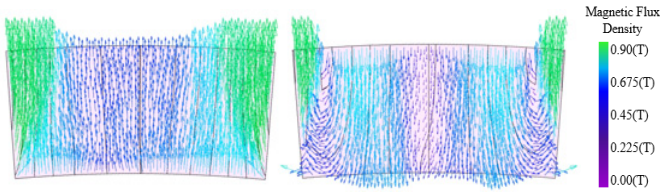

(**a**) (**b**)

Figure 7. Magnetization direction of LCF PM for VM to PMSM: (**a**) VM; (**b**) PMSM.

3.1. Flux Enhancing in VM

The DWFMM performs Flux Enhancing to improve torque compared to the SWFMM's VM operation. Figure 8 shows the Magnetic Equivalent Circuit of Flux Enhancing in the DWFMM's VM operation. For HCF PM and LCF PM, assuming that the steel laminated to the rotor and stator in the open circuit has infinite permeability and no leakage magnetic flux, the magnetic flux of VM can be expressed as Equation (3):

$$\phi_{VM} = \frac{F_{HM}(2R_g + R_r + R_s + R_{LM}) + F_{LM}(2R_g + R_r + R_s + R_{HM})}{(2R_g + R_r + R_s + R_{HM})(2R_g + R_r + R_s + R_{LM})} \quad (3)$$

where ϕ_{VM}, F_{HM}, F_{LM}, R_g, R_r, R_s, R_{HM}, and R_{LM} are the magnetic flux of VM, MMF of HCF PM, LCF PM, reluctance of air gap, rotor, stator, HCF PM, and LCF PM, respectively. According to the magnetic flux lines of the VM, when DC flows through Coil 3 of the slave winding, the magnetic flux increases. The added magnetic flux by DC for Flux Enhancing can be expressed as Equation (4).

$$\phi_{DC} = \frac{2F_{DC}(2R_g + R_r + R_s + R_{LM}) + 2F_{DC}(2R_g + R_r + R_s + R_{HM})}{4(2R_g + R_r + R_s + R_{HM})(2R_g + R_r + R_s + R_{LM})} \quad (4)$$

where ϕ_{DC} and F_{DC} are the magnetic flux and MMF by DC. Figure 9 shows the increase in magnetic flux with the DC of the SWFMM and DWFMM. The magnetic flux by DC of Equation (4) was added to the magnetic flux of the VM of Equation (3), and accordingly, the magnetic flux was increased in Flux Enhancing. By excluding F_{DC} from the equation for ϕ_{DC}, the magnetic flux becomes identical to the magnetic flux of the SWFMM, making the Zero Flux the same as the flux of the SWFMM.

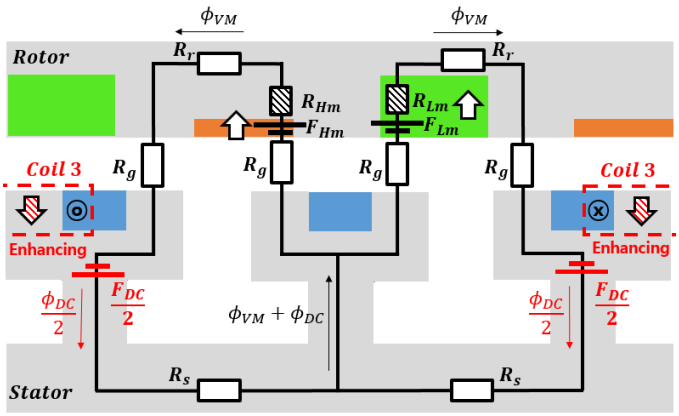

Figure 8. Magnetic Equivalent Circuit of Flux Enhancing in VM.

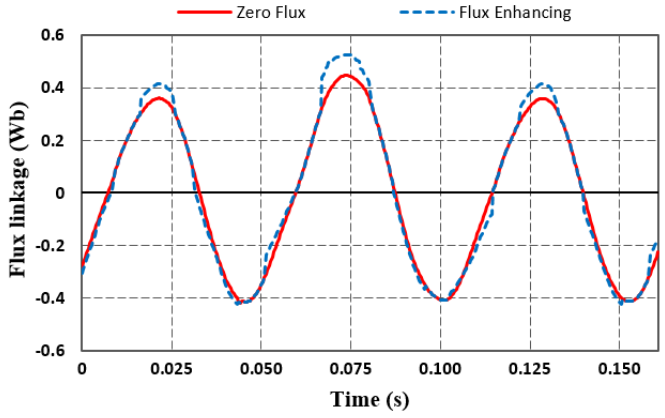

Figure 9. Flux linkage of Flux Enhancing in VM.

Also, Figure 10 shows that the magnetic flux density of the LCF PM increases before and after Flux Enhancing in VM. If the DC of Flux Enhancing does not match the magnetic flux line of the VM operation of the DWFMM, demagnetization of the LCF PM may result, which may decrease the performance of the DWFMM. Therefore, Flux Enhancing is partially performed for the demagnetization of the LCF PM.

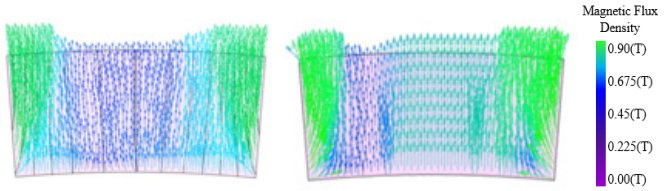

(**a**) (**b**)

Figure 10. Magnetic flux density of LCF PM with Flux Enhancing in VM: (**a**) Zero Flux; (**b**) Flux Enhancing.

3.2. Flux Weakening in PMSM

Generally, the back EMF is proportional to speed. In the PMSM mode operation of the SWFMM, which is used at high speeds, the machine has a high terminal voltage. This high terminal voltage necessitates the use of a high-capacity inverter and leads to speed limitations. The DWFMM uses a slave winding to lower the terminal voltage by using flux weakening in the PMSM. Figure 11 shows the Magnetic Equivalent Circuit during the PMSM operation of the DWFMM. The magnetic flux of the PMSM can be expressed as Equation (5).

$$\phi_{PMSM} = \frac{F_{HM} + F_{LM}}{(2R_g + R_r + R_s + R_{HM} + R_{LM})} \tag{5}$$

where ϕ_{PMSM} is the magnetic flux of the PMSM. The DC for flux weakening flows through slave winding coil 1 and 2 in the opposite direction to the magnetic flux line. The added magnetic flux by DC for flux weakening can be expressed as Equation (6).

$$\phi_{DC} = \frac{2F_{DC}}{(2R_g + R_r + R_s + R_{HM} + R_{LM})} \tag{6}$$

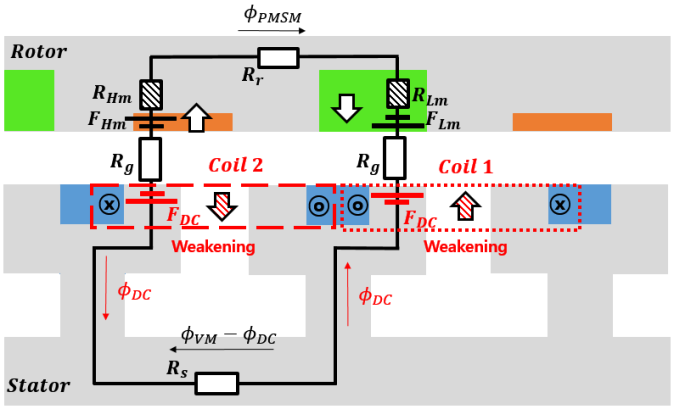

Figure 11. Magnetic Equivalent Circuit of flux weakening in PMSM.

Accordingly, Figure 12 shows the magnetic flux is lowered and the terminal voltage is reduced during flux weakening in the PMSM. Similar to Flux Enhancing, Zero Flux is the same as the flux of the SWFMM.

Figure 13 shows the magnetic flux density of the LCF PM before and after Flux Weakening, and in Figure 13b, the magnetic flux density decreases.

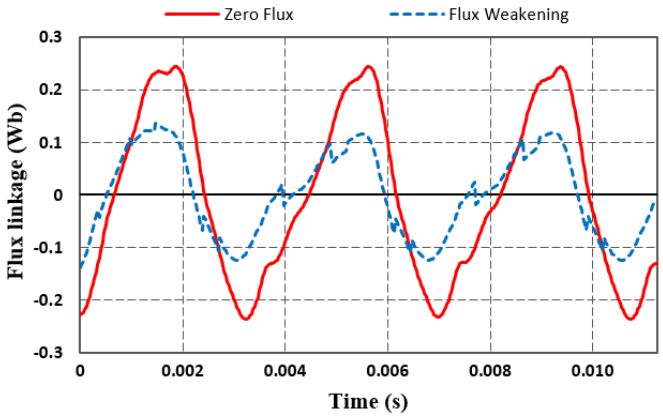

Figure 12. Flux linkage of Flux Weakening in PMSM.

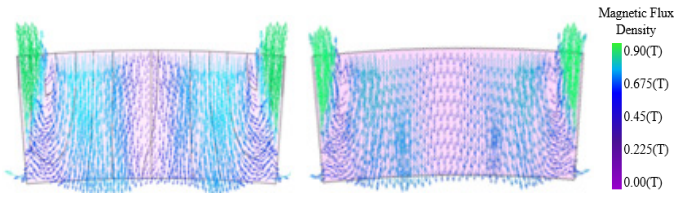

(**a**) (**b**)

Figure 13. Magnetic flux density of LCF PM with Flux Weakening in PMSM: (**a**) Zero Flux; (**b**) Flux Weakening.

4. Comparison of Performance for Washing Machine

Generally, the washing operation is performed at a low-speed operation. Therefore, the SWFMM and DWFMM are operated as a VM. In this case, the SWFMM is designed targeting a typical washing machine, and the parameters of the SWFMM are those of the washing machine. Accordingly, the SWFMM and DWFMM are compared at 50 RPM, the typical speed used for washing operation. Figure 14 shows that the torque of the DWFMM is higher than that of the SWFMM during low-speed operation. The average torque value of the SWFMM was 16.05 Nm. Also, the DWFMM used a DC of 5 A for Flux Enhancing in the VM, and the average torque value was 16.87 Nm. The torque value increased by about 4.91% compared to the SWFMM. Due to the low-speed operation, the DWFMM terminal voltage was very low, about 65 V_{pk}. This means that it is independent of the inverter rating limit when operating the washing operation. In addition, the torque can be improved by adjusting the magnetic flux according to the DC value. Table 2 shows the FEM results for the washing operation of the two machines.

Table 2. FEM analysis results and comparison in washing operation.

Machine Type Operating Mode	Unit	SWFMM VM	DWFMM Flux Enhancing
Speed	Rpm	50	50
Master Current	A	1.7	1.7
Slave Current	A	-	10
Torque	Nm	16.08	16.87
Rate of Increase Torque	%	-	4.91

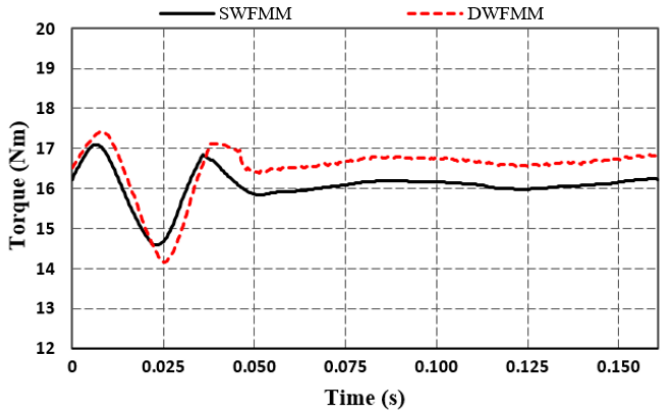

Figure 14. A torque comparison of the SWFMM and DWFMM for the washing operation (50 RPM).

The dehydration operation of washing machines is generally performed at high speeds. Therefore, both the SWFMM and DWFMM operated as the PMSM. The two machines were compared at a typical speed of 1400 RPM used for dehydration operation. Figure 15 shows that the phase voltage of the DWFMM is lower than that of the SWFMM during high-speed operation. The terminal voltage of the SWFMM is 681 V_{pk}, while the phase voltage of the DWFMM is 449 V_{pk}. As a result of comparing the two machines, the terminal voltage was reduced by about 34%. In addition, terminal voltage can be adjusted according to the value of the DC for Flux Weakening. Reducing the phase voltage can lower the inverter rating, increasing the maximum speed. Table 3 shows the FEM results for the dehydration operation of the two machines.

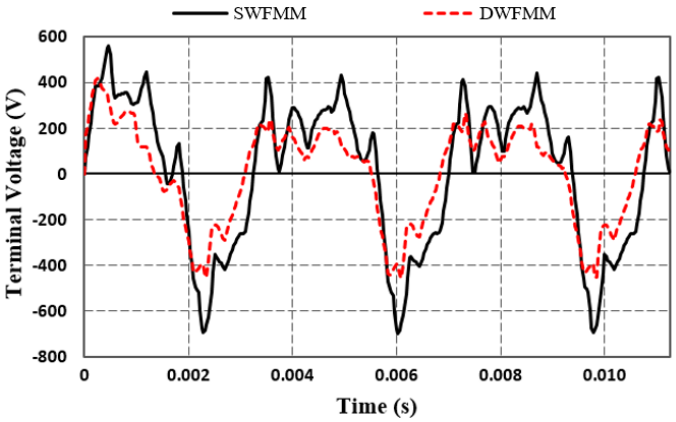

Figure 15. Terminal voltage comparison of SWFMM and DWFMM for dehydration operation (1400 RPM).

Table 3. FEM analysis results and comparison in dehydration operation.

Machine Type Operating Mode	Unit	SWFMM PMSM	DWFMM Flux Weakening
Speed	Rpm	1400	1400
Master Current	A	1.5	1.5
Slave Current	A	-	10
Terminal Voltage	Vpk	681	449
Rate of Decrease Voltage	%	-	34.06

5. Conclusions

In this paper, we propose a topology of the DWFMM for performance-enhanced variable speed application machines. The DWFMM is a dual winding machine that uses

the master winding in the slots of the SWFMM and the slave winding in the modulation poles. The master winding is for the general operation of the machine, while the slave winding serves two purposes. First, it performs the pole-changing operation to switch between the Vernier Mode and the PMSM Mode of the DWFMM. Second, it adjusts the flux in both modes by either enhancing or weakening it. The proposed DWFMM was analyzed using FEM analysis and evaluated through a comparison with the SWFMM under the same application conditions. In the Vernier Mode, the DWFMM utilized Flux Enhancing, resulting in increased torque during the washing operation compared to the SWFMM. Additionally, in the PMSM Mode, the DWFMM employed Flux Weakening, which resulted in a lower phase voltage during the dehydration operation compared to the SWFMM. This indicates that the DWFMM can operate with a smaller capacity inverter or at higher speeds. The DWFMM could be suitable for next-generation washing machines and variable speed application machines that meet these requirements. Future research should focus on Deterministic Design Optimization and Robust Design Optimization processes to enhance the performance and efficiency of the model. The optimization model should target parameters such as the magnetization degree, torque, and efficiency of the permanent magnets. Moreover, based on the optimized model, it is necessary to conduct studies to verify the control accuracy of pole changing by controlling the position of the LCF PM using an encoder. This involves deriving magnetization rate calculation formulas based on back EMF waveforms and magnitudes and proving the control accuracy through pole-changing experiments.

Author Contributions: Conceptualization, M.-G.L. and S.-H.L.; methodology, M.-G.L.; software, M.-G.L.; validation, M.-G.L. and S.-H.L.; formal analysis, M.-G.L.; investigation, M.-G.L. and S.-H.L.; data curation, M.-G.L. and S.-H.L.; writing—original draft preparation, M.-G.L.; writing—review and editing, M.-G.L., K.-Y.H. and S.-H.L.; visualization, M.-G.L.; supervision, K.-Y.H.; project administration, S.-H.L.; funding acquisition, M.-G.L. All authors have read and agreed to the published version of the manuscript.

Funding: This work was supported by the Korea Evaluation Institute of Industrial Technology (KEIT) and the Ministry of Trade, Industry, and Energy (MOTIE) of the Republic of Korea (No. 20012815).

Data Availability Statement: The data presented in this study are available on request from the corresponding author.

Conflicts of Interest: The authors declare no conflicts of interest.

References

1. Jin, C.S.; Jung, D.S.; Kim, K.C.; Chun, Y.D.; Lee, H.W.; Lee, J. A study on improvement magnetic torque characteristics of IPMSM for direct drive washing machine. *IEEE Trans. Magn.* **2009**, *45*, 2811–2814.
2. Lee, D.M.; Lim, D.C.; Ahn, H.J. Position linearisation scheme for permanent magnet synchronous motor drive of washing machine using low-resolution hall sensors. *Electron. Lett.* **2015**, *51*, 1765–1767. [CrossRef]
3. Chi, S.; Zhang, Z.; Xu, L. Sliding-mode sensorless control of directdrive PM synchronous motors for washing machine applications. *IEEE Trans. Ind. Appl.* **2009**, *45*, 582–590. [CrossRef]
4. Kim, B.; Lipo, T.A. Operation and Design Principles of a PM Vernier Motor. *IEEE Trans. Ind. Appl.* **2014**, *50*, 3656–3663. [CrossRef]
5. Kim, B.; Lipo, T.A. Analysis of a PM Vernier Motor with Spoke Structure. *IEEE Trans. Ind. Appl.* **2016**, *52*, 217–225. [CrossRef]
6. Kim, B. Characteristic analysis of a vernier PM motor considering adjustable speed control. In Proceedings of the 2016 IEEE Transportation Electrification Conference and Expo, Asia-Pacific (ITEC Asia-Pacific), Busan, Republic of Korea, 1–4 June 2016; pp. 671–676.
7. Choi, M.; Kim, B. Calculation of PM Vernier Motors Using an Improved Air-Gap Permeance Function. *IEEE Trans. Magn.* **2019**, *55*, 1–5. [CrossRef]
8. Baloch, N.; Kwon, B.I. Surface Permanent Magnet Pole Changing Vernier Machine. Korean Patent 10-1970398, 12 April 2019.
9. Yang, H.; Lin, H.; Zhu, Z.Q.; Lyu, S. Influence of magnet eddy current on magnetization characteristics of variable Flux memory machine. *AIP Adv.* **2018**, *8*, 056602. [CrossRef]
10. Yang, H.; Zhu, Z.Q.; Lin, H.; Wu, D.; Hua, H.; Fang, S.; Huang, Y.-K. Novel High-Performance Switched Flux Hybrid Magnet Memory Machines with Reduced Rare-Earth Magnets. *IEEE Trans. Ind. Appl.* **2016**, *52*, 3901–3915. [CrossRef]
11. Yang, H.; Zhu, Z.Q.; Lin, H.; Xu, P.L.; Zhan, H.L.; Fang, S.; Huang, Y. Design Synthesis of Switched Flux Hybrid-Permanent Magnet Memory Machines. *IEEE Trans. Energy Convers.* **2017**, *32*, 65–79. [CrossRef]

12. Yang, H.; Zhu, Z.; Lin, H.; Fang, S.; Huang, Y. Synthesis of Hybrid Magnet Memory Machines Having Separate Stators for Traction Applications. *IEEE Trans. Veh. Technol.* **2018**, *67*, 183–195. [CrossRef]
13. Zhou, Y.; Chen, Y.; Shen, J. Analysis and Improvement of a Hybrid Permanent Magnet Memory Motor. *IEEE Trans. Energy Convers.* **2016**, *31*, 915–923. [CrossRef]
14. Hua, H.; Zhu, Z.Q.; Pride, A.; Deodhar, R.P.; Sasaki, T. A Novel Variable Flux Memory Machine with Series Hybrid Magnets. *IEEE Trans. Ind. Appl.* **2017**, *53*, 4396–4405. [CrossRef]
15. Zhu, Z.Q.; Hua, H.; Pride, A.; Deodhar, R.; Sasaki, T. Analysis and reduction of unipolar leakage Flux in series hybrid permanent-magnet variable Flux memory machines. *IEEE Trans. Magn.* **2017**, *53*, 1–4. [CrossRef]
16. Li, F.; Chau, K.T.; Liu, C. Pole-Changing Flux-Weakening DC-Excited Dual Memory Machines for Electric Vehicles. *IEEE Trans. Energy Convers.* **2016**, *31*, 27–36. [CrossRef]
17. Wang, D.; Lin, H.; Yang, H.; Zhang, Y.; Lu, X. Design and Analysis of a Variable-Flux Pole-Changing Permanent Magnet Memory Machine. *IEEE Trans. Magn.* **2015**, *51*, 1–4.
18. Li, F.; Chau, K.T.; Liu, C.; Qiu, C. New Approach for Pole-Changing with Dual-Memory Machine. *IEEE Trans. Appl. Supercond.* **2014**, *24*, 1–4.
19. Baloch, N.; Kwon, B.I. A pole changing vernier machine with consequent pole rotor. *Int. J. Appl. Electromagn. Mech.* **2019**, *59*, 931–941. [CrossRef]
20. Chung, S.U.; Moon, S.H.; Kim, D.J.; Kim, J.M. Development of a 20-Pole–24-Slot SPMSM with Consequent Pole Rotor for In-Wheel Direct Drive. *IEEE Trans. Ind. Electron.* **2016**, *63*, 302–309. [CrossRef]
21. Onsal, M.; Demir, Y.; Aydin, M. A New 9-Phase Permanent Magnet Synchronous Motor with Consequent Pole Rotor for High Power Traction Applications. *IEEE Trans. Magn.* **2017**, *53*, 1–6. [CrossRef]
22. Yang, H.; Lin, H.; Fang, S.; Huang, Y.; Zhu, Z.Q. A novel stator-consequent-pole memory machine. In Proceedings of the 2016 IEEE Energy Conversion Congress and Exposition (ECCE), Milwaukee, WI, USA, 18–22 September 2016; pp. 1–8. [CrossRef]
23. Lee, S.-H.; Baloch, N.; Kwon, B.-I. Design and Analysis of a Double Consequent Pole Changing Vernier Machine. *Int. J. Appl. Electromagn. Mech.* **2020**, *64*, 941–949. [CrossRef]
24. Lee, S.-H.; Kwon, J.-W.; Kwon, B.-I. Improving Efficiency of a Pole-Changing Vernier Machine Considering Residual Magnetic Flux Density. *Energies* **2023**, *16*, 6707. [CrossRef]
25. Hwang, K.-Y.; Yoon, K.-Y. Improvement of Braking Response Performance of Fault-Tolerant Dual Winding Motor for Integrated Brake System Using Winding Switching. *Appl. Sci.* **2023**, *13*, 3442. [CrossRef]